Proceedings of IWHT2013

2nd International Workshop on Heat Transfer Advances for Energy Conservation and Pollution Control
October 18-21, 2013, Xi'an, China

IWHT2013-083

Improved thermal properties of paraffin wax by the addition of TiO_2 nanoparticles

Jifen Wang[a,b,*], Huaqing Xie[a], Zhixiong Guo [b], Yang Li[a]

[a]School of Urban Development and Environmental Engineering, Shanghai Second Polytechnic University, Shanghai 201209, China
[b]Department of Mechanical and Aerospace Engineering, Rutgers, The State University of New Jersey, Piscataway, NJ 08854-8058, USA

(*Corresponding Author: wangjifen@edu.sspu.cn)

Abstract

TiO_2 nanoparticles about 20 nm in diameter in the form of anatase were prepared and characterized by various analytical methods. The nanoparticles were successfully dispersed into a paraffin wax (PW) matrix without any surfactant. The differential scanning calorimetric instrument and transient short hot wire method were used to measure the thermal properties of the TiO_2/PW composites. It is found that the phase change temperature varies with adding TiO_2 nanoparticles into the PW matrix. The composites have a decreased latent capacity for both solid-solid and solid-liquid phase changes, except for the case with 1.0 wt% TiO_2 nanoparticles loading. The latent capacity of the 1.0 wt% TiO_2/PW composite is higher than that of the virgin PW by 8.3 J/g for solid-solid phase change and by 27.5 J/g for solid-liquid phase change, respectively. The thermal conductivity of the composites is substantially augmented, and it increases with increasing TiO_2 mass fraction at the tested temperatures. With temperature increase the composite changes from solid to liquid and the thermal conductivity of the composite decreases.

Keywords: Phase-change composites; Thermal conductivity; Latent heat; Paraffin wax; TiO_2 nanoparticles

1 Introduction

Nanoparticles exhibit remarkably different physical and chemical properties from their bulk form [1, 2]. They can be used in many ways of innovations that would be very useful for mankind. In recent years, various sorts of nanoparticles can be produced because of the rapid advance in nanotechnology [3, 4], greatly promoting the innovation in pharmaceutical engineering [5], mechanical engineering [6], electronic engineering [7], and other industrial processes [8]. For example, nanoparticles are used in thermal management to enhance the thermal conductivity of matrix materials [9]. The high conductivity of metal and/or metal oxide nanoparticles is used to improve the heat transfer of generally low-conductivity fluids in mini- and micro-scale heat exchangers, such as in electronic devices and high capacity military communication devices [10-12].

Recently, He et al. [13] prepared water-based TiO_2 nanofluids and measured their thermal conductivities. Results showed that when the particle concentration increased, the thermal conductivity of the nanofluid increased to a level greater than the prediction of the Hamilton-Crosser model [14,15]. The smaller the particles size is, the higher is the thermal conductivity. Murshed et al. [16] measured the thermal conductivity of different nanofuids consisted of Al_2O_3/water, Al_2O_3/ethylene glycol, TiO_2/water and TiO_2/ethylene glycol, respectively. They found that the nanofluids had a higher thermal conductivity than respective base fluids and the increase in thermal conductivity varied with the nanoparticle concentration level as well as temperature. Xie et al. [17] revealed that the thermal conductivity of Al_2O_3 nanofluid was higher than that of the base fluid and increased with increasing nanoparticle concentration level. The enhanced thermal conductivity ratio decreases with an increase in pH value, from pH 2.0 to pH 11.5. They also found that the thermal conductivity of nanofluids varied with particle size and the optimal particle size for thermal conductivity enhancement was 60 nm.

Due to thermal energy storage can be used to enhance energy efficiency and to improve energy conservation and management, studies of thermal energy storage materials have been attracting more and more attention from all over the word. Thermal energy storage materials can be categorized into sensible heat storage materials, latent heat storage materials and thermal chemical materials. Latent heat thermal energy storage uses phase change materials (PCMs) that have much higher heat storage density and extremely smaller temperature variation during phase change process, compared with sensible heat storage materials. In comparison with chemical thermal materials and inorganic PCMs, organic PCMs have a proper phase change temperature range, little or no super cooling, lower vapor pressure, nontoxicity, noncorrosivity, and excellent thermal stability. Therefore, PCM is one of the most preferred

forms of thermal energy storage and has promising applications in the field of solar energy storage, industrial waste energy storage, etc.

Fatty acids and paraffin wax (PW) are good organic PCMs [18-20] due to their desirable characteristics such as high latent heat of fusion, negligible super cooling, low vapor pressure in the melt, and stability. However, the low thermal conductivity of fatty acids and n-alkanes is a major drawback, decreasing the rates of heat storage and retrieval during melting and crystallization processes, which in turn limiting their utility areas. Due to the improved thermal properties, fluids with metal and metal oxide particles were commonly used to enhance heat transfer in energy conversion and management systems [9, 21, 22]. Therefore, studies have been carried out to develop latent heat thermal energy storage systems with enhanced thermal performance, like dispersing high conductivity particles and inserting a metal matrix into fatty acids [23, 24]. In spite of the increased thermal conductivity, the relatively "big" particles in the organic matrix can be easily separated out from the composite. However, nanoparticles can remain separate in the composite because of their Brown' motion in liquid. Recent advances of nanotechnology make it possible to exploit the development of stable organic phase-change composites.

In this study, TiO_2 nanoparticles are carefully prepared from $TiCl_4$ hydrolysis reaction and characterized by various analytical methods. The nanoparticles are then applied into a PW matrix to make phase change composites. The thermal properties of the composites including melting point, latent heat capacity, and thermal conductivity at both solid and liquid states are investigated in detail.

2 Experimental description

2.1 Sample preparation

The PW (industrial grade) with melting temperature of 48~50 ^oC, titanium tetrachloride ($TiCl_4$), and other relative chemical reagents were obtained from Sinopharm Chemical Reagent Co. Ltd and directly used in the present experiments without further purification.

In the procedure of the hydrolysis reaction, 1ml $TiCl_4$ was dropped into 20 ml solution of hydrogen chloride with stirring in an ice-bath. Then 2 ml ammonium solution was added into the mixture to consume the excess hydrogen chloride, and the mixture was stirred for 30 min at room temperature. After that, the temperature of the mixture was increased to 90 ^oC and kept stirring for 60 min. Ammonia was dropped into the mixture until the pH of the mixture reached to 6. Without heating and stirring the mixture was cooled down to room temperature naturally for about 8 hrs. The mixture after reaction was diluted by distilled water, filtered, and washed repeatedly until the washings showed no presence of Cl^- ions. The cleaned solid was collected and dried at 600 ^oC for 3 hrs and the dried powder consisted of TiO_2 nanoparticles. The chemical reactions in the processes are as follows:

$$\begin{aligned} TiCl_4 + H_2O &= TiOH^{3+} + H^+ + 4Cl^- \\ TiOH^{3+} &= TiO^{2+} + H^+ \\ TiO^{2+} + H_2O &= TiO_2 + 2H^+ \end{aligned} \quad (1)$$

The fabricated TiO_2 nanoparticles were finally added into the melting PW in a mixing container. The mixture was subjected to intensive sonication for 30 min at 65 ^oC to make TiO_2/PW composites.

2.2 Characterization of the particles

Various analytical methods have been applied to characterize the TiO_2 nanoparticles. Dry TiO_2 nanoparticles were analyzed without any treatment if not specified. Scanning electron microscopy (SEM) observation was performed on a Hitachi S-4800 field emission SEM device. The sample was put on a piece of silicon and set under the instrument to be observed and pictured. Transmission electron microscopy (TEM) pictures were taken on a JEOL 2100F high resolution TEM device. The sample was scattered onto a copper mesh and observed directly under the instrument. Fourier transformation infrared (FTIR) spectra were collected on a Bomem DA 8 spectrometer. 1 mg of the sample was mixed with about 200 mg KBr crystal in a container and pressed into tablet by a press tools for tablets. The tablet was put into the device and detected from 4000 cm^{-1} to 400 cm^{-1}. X-ray diffraction (XRD) patterns were recorded on a D8-Advance diffractometer using Cu Kα X-ray at 40 kV and 100 mA. The sample was put into a solid sample box and set onto the slot of the machine. The 2θ of XRD was scanned from 10^o to 90^o.

2.3 DSC analysis

The thermal properties including the melting temperature and latent heat capacity of both the pure PW and TiO_2/PW composites were measured using a differential scanning calorimetric (DSC) instrument (Diamond DSC, Perkin Elmer, USA). Indium was used as a reference for temperature calibration. Sample with mass of 3.00 ~5.00 mg was placed and pressed into crucibles at room temperature. A lid was placed on the sample to make excellent thermal contact between the sample and the crucible. Then the crucible containing the sample was put into the DSC instrument in shielding nitrogen gas flow of 20 ml/min. After 1 min remaining at the initial temperature, the DSC measurements were performed at a linear heating rate of 5 $^oC\ min^{-1}$ in a temperature range from 15 ^oC to 65 ^oC. The temperature was maintained at 65 ^oC for 1 min to remove thermal history, and then cooled down to 15 ^oC.

2.4 Thermal conductivity measurement

The thermal conductivities (k) of the pure PW and the TiO_2/PW composites were measured by a transient short-hot-wire method, and determined by the following formula [25]:

$$k = \left(\frac{q}{4\pi}\right) \Big/ \frac{d(\theta(\tau))}{d(\ln\tau)} \quad (2)$$

where q, τ and $\theta(\tau)$ are the applied heating power per unit length, the heating time, and the temperature rise of the hot-wire, respectively. Initially the platinum wire immersed in the PW or composite was at equilibrium with the surroundings. The uncertainty of this measurement is estimated to be ±2.0% and the detailed estimation was available in reference [26]. For the thermal conductivity measurements, PCM sample was melted and poured into a stainless steel cylinder container. A platinum wire with a diameter of 70 μm and a thermocouple were immersed in the PCM to record and test the temperature of the

PCM before a waterproof lid covered the container. The platinum wire served as both a heating unit (hot wire) and an electrical resistance thermometer. The container was put into a water bath with specified test temperatures of 20 ^{o}C. When the thermocouple in the PCM showed a temperature vibration less than 0.1 ^{o}C for 10 min, the hot wire in the sample started to probe. The hot wire probe was subjected from time t=0 to a step change in the electrical current applied to the wire. Then the temperature was increased to 40 ^{o}C and 60 ^{o}C, respectively, to repeat the above steps. For each the test temperature, three measurements were conducted and the average value was taken.

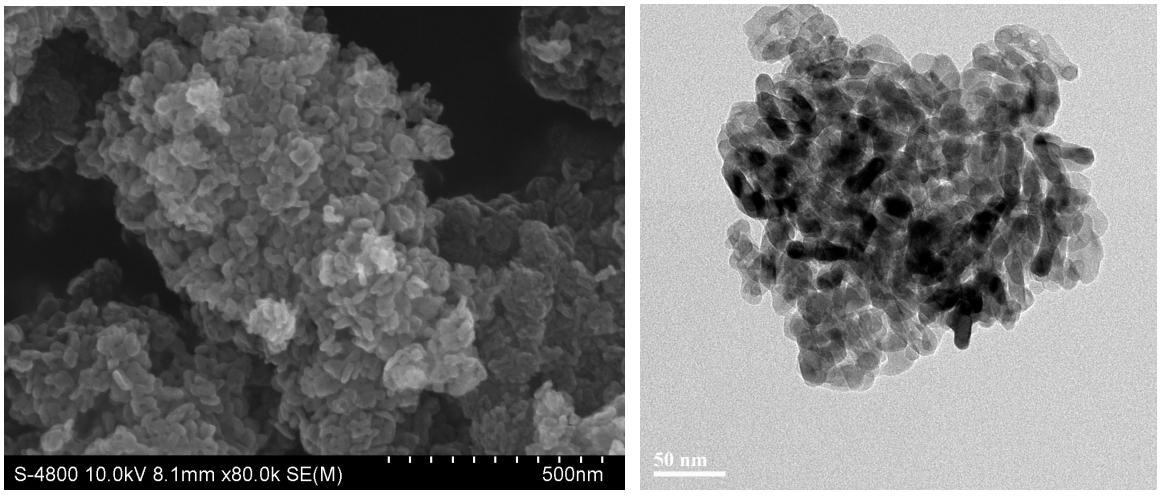

Figure 1 SEM (left) and TEM (right) images of our fabricated TiO_2 particles

3 Results and discussion

3.1 Analysis of the TiO_2 particles

Figure 1 shows the SEM and TEM images of the fabricated TiO_2 particles. Via observation the size of the nanoparticles is estimated smaller than 30 nm in diameter. The particles are columnar in the shape. The nanoparticles clustered into groups because of the high surface energy with so small size.

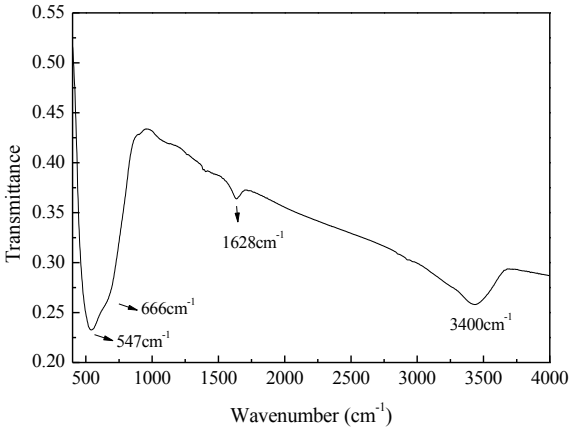

Figure 2 FTIR spectrum of the TiO_2 particles

Figure 2 presents the FTIR spectrum of the TiO_2 particles. The band at 547 cm^{-1} corresponds to the characteristic of band stretching vibration of Ti-O, and it shifts to longer wavenumber compared with the bulk TiO_2 (540 cm^{-1}). The band transmitted at 666 cm^{-1} can be attributed to the characteristic of anatase form of TiO_2 and it red shifts 6cm^{-1} than the big crystal because of the incomplete crystal in the nano size. The band at 1628 cm^{-1} and the broad band of 3400 cm^{-1} correspond to the characteristic of the O-H stretching of the water in the sample because the water combined in the sample couldn't be removed completely in the current synthesis conditions.

Figure 3 shows the XRD spectrum of the TiO_2 particles. XRD is an important method to analyze the structure of materials, especially for determining the phase of the crystalline. The spectrum clearly indicates that the particles are in the anatase form. Anatase characteristics are shown at 25.3^{o} (101), 38^{o} (004), 48^{o} (200), 54^{o} (105), 62.5^{o} (204), and 70.3^{o} (220). No impurity elements could be detected within the detection capability. The average diameter of the nanoparticles is about 20 nm calculated by the XRD data.

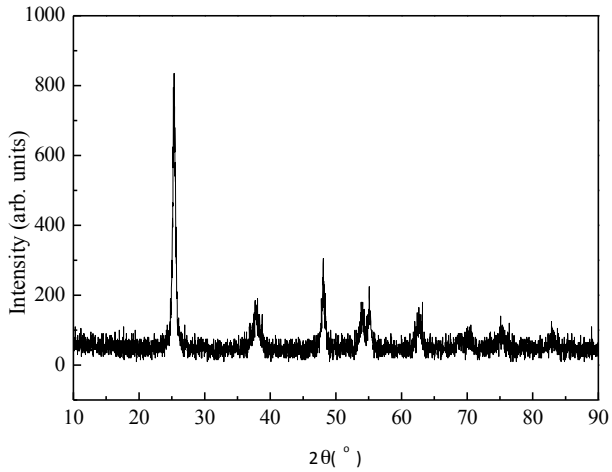

Figure 3 XRD spectrum of the TiO_2 particles

3.2 DSC analysis of the composites

It is of paramount importance to investigate the phase change temperature and latent heat capacity of PCM. For PW,

the molecules of PW will rotate and rearrange when it absorbs heat at a certain temperature in solid state. The transition of the microstructure of PW from a compact solid state into a loose one indicates the occurrence of solid-solid phase change. When the temperature is further raised up to the melting point, the molecules of PW will absorb latent heat and convert into kinetic energy to overcome the intermolecular forces and the PW will turn into liquid state. In this work, DSC analysis was conducted to investigate the influences of the addition of TiO_2 particles on the phase change temperature and the latent heat storage capacity of the TiO_2/PW composites.

Figure 4 displays the DSC thermograms of the TiO_2/PW composites with different particle concentration levels. The peaks on a DSC curve represent the phase change behavior of a PCM. As shown on the figure, the TiO_2/PW composites have almost the same shape of curves with the virgin PW. There are two main peaks in each curve. The big one to the right-hand side is the melting peak and the one to the most left-hand side is attributed to solid-solid phase change. The small peak following the solid-solid phase change peak might be the transitionary structure during phase change process.

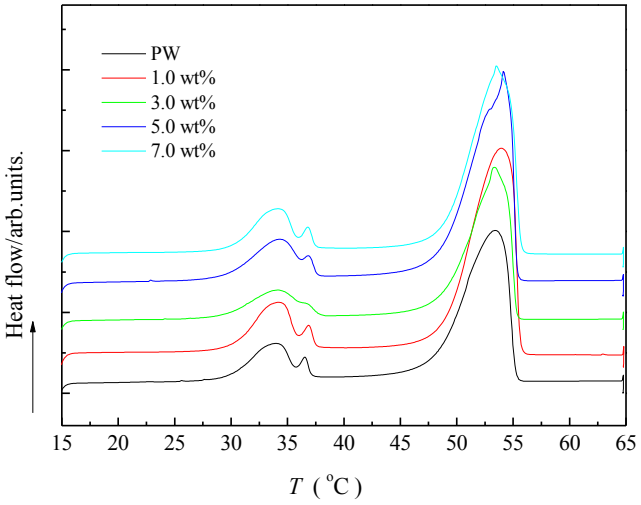

Figure 4 DSC curves of the composites

In order to study how the phase change point and the latent heat capacity of the composites vary with the loading of TiO_2 particles, the latent heat capacity and the phase change point data were summarized in the table 1, where L_{s-s} and L_s represent latent heat capacity of solid-solid phase change and latent heat capacity of solid-liquid phase change of the PCM, respectively; T_{s-s} and T_m represent the solid-solid phase change temperature and solid-liquid phase change temperature, respectively. In this study, the phase change temperature is taken as the onset temperature of phase change on the DSC curves; and it is obtained as the temperature of intersection point between the tangent of the DSC curve at half height of the peak and the baseline. Therefore, the onset temperature is lower than the peak temperature on the melting DSC curve. It is seen that T_{s-s} of the composites shifts to low temperature compared with that of the virgin PW, while T_m of the composites shifts to high temperature; and they increase with increasing the loading of the TiO_2 particles. For the latent heat capacity, both L_{s-s} and L_s in the TiO_2/PW composites reduce, compared with those for the PW, except for the composite with 1.0 wt% TiO_2 loading. L_{s-s} of the 1.0 wt% TiO_2/PW (39.0 J/g) is 8.3J/g higher than that of the PW. L_s of the 1.0 wt% TiO_2/PW (165.3J/g) is 27.5J/g higher than that of the PW. In general, there are at least two factors that cause the latent capacity change in the composite. One is the interaction between the PW molecules and TiO_2 particles, which will increase the latent capacity of the composites [27, 28]. The other one is that the addition of the TiO_2 particles would reduce the latent heat capacity of the composites because the replacement of nanoparticles for the PW molecules could lead to absorb or release more energy during composite melting or solidification processes. So the latent heat capacity of the composite would increase when the first factor is stronger than the second one and vice versa.

Table 1 Melting temperature and latent heat capacity of PW and TiO_2/PW composites

PCMs	T_{s-s} (°C)	L_{s-s} (J/g)	T_m (°C)	L_s (J/g)
PW	30.1	30.7	48.6	137.8
1.0 wt%	29.6	39.0	48.7	165.3
3.0 wt%	30.0	28.2	50.4	134.0
5.0 wt%	29.9	28.2	50.4	130.0
7.0 wt%	29.7	28.3	51.4	124.0

3.3 Thermal conductivity of the composites

The thermal conductivity is an important property of PCMs because the rate of energy storage or release is highly depended on the thermal conductivity of materials. PCMs are used for thermal energy storage in environments with temperature variation. Therefore, it is important to know the thermal conductivity of the PCMs in both solid and liquid states of the temperature range of interest. We measured the thermal conductivity of the composites at different temperatures to show how the thermal conductivity changes with temperature and phase state. The major test temperatures are 20 °C, 40 °C and 60 °C, respectively. At 20 °C, the composite is in the solid state prior to solid-solid phase change. At 40 °C, it is located between solid-solid phase change and solid-liquid phase change. At 60 °C, the composite is in the liquid state. So these three temperature points present three phases of the PCM studied.

Figure 5 depicts the dependence of the thermal conductivity of the TiO_2/PW composites on the TiO_2 loadings in the three test temperatures. In the figure, k and ϕ_w represent the thermal conductivity of the PCM and the mass ratio of TiO_2 nanoparticles in the composites, respectively. The discrete symbols represent experimental measurements and the dotted lines are from theoretical prediction. For the three test temperatures, it is seen that k decreases with increasing temperature; but increases with increasing loading of the TiO_2 nanoparticles. However, the enhancement of the thermal conductivity in measurements is lower than the theoretical estimated result, in particular at higher loadings over 3 wt%. It is well known that the nanoparticles are easy to be aggregated and it is difficult to separate the aggregation into individual

particles in the composite. This is one fact why the experimental measurement is lower than the theoretical prediction. Interfacial thermal resistance between the nanoparticles and the matrix molecules can be accounted as a dominant fact for the discrepancy [29].

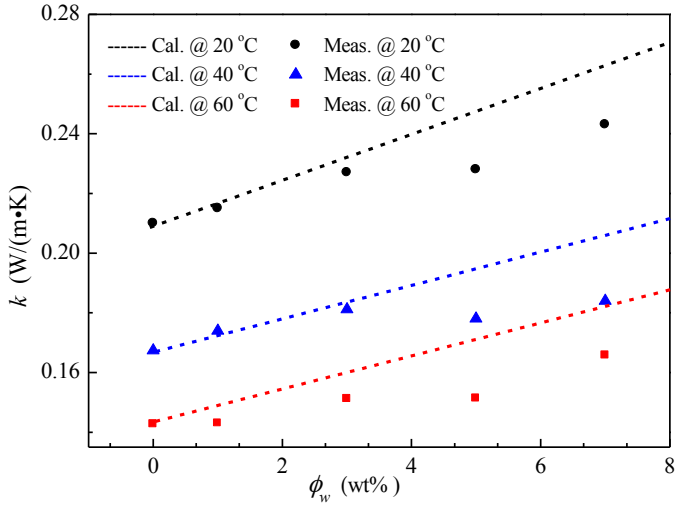

Figure 5 Thermal conductivity vs. TiO_2 mass loading percentage

Many theoretical works had carried out to estimate the thermal conductivity of composite. The equation used to calculate the thermal conductivity of the composite for Fig. 5 is as follows [30]:

$$k_c=\Phi_v\times k_p+(1-\Phi_v)\times k_f \quad (3)$$

where Φ_v is the particle volume fraction in the composite; and k_c, k_p and k_f are thermal conductivities of the composite, the nanoparticle and the matrix, respectively. The relationship between volume fraction and weight fraction Φ_w is

$$\Phi_v = (m_p\times\rho_c)/(m_c\times\rho_p) =\Phi_w\times(\rho_c/\rho_p). \quad (4)$$

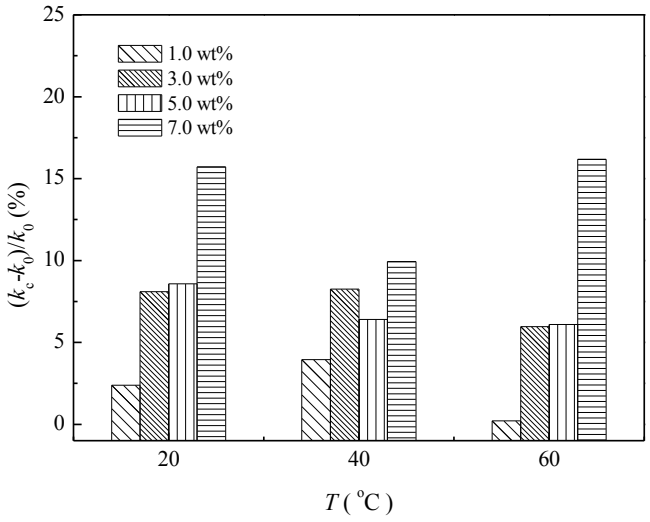

Figure 6 Enhancement percentage of thermal conductivity for the four different loadings at the three test temperatures

Figure 6 shows the thermal conductivity enhancement percentages subjected to different TiO_2 mass ratios at the test temperatures. In the figure, k_c and k_0 represent the thermal conductivities of the composites and pure PW, respectively. It is seen that the thermal conductivity enhancement of the composites has an increase trend with the loading of TiO_2 nanoparticles at both 20 °C and 60 °C. At 40 °C, the thermal conductivity enhancement ratio of the composite with 3.0 wt% TiO_2 nanoparticles is higher than that with 5.0 wt% TiO_2 nanoparticles. It might be caused by the nanoparticles being into groups in 5.0 wt% composite.

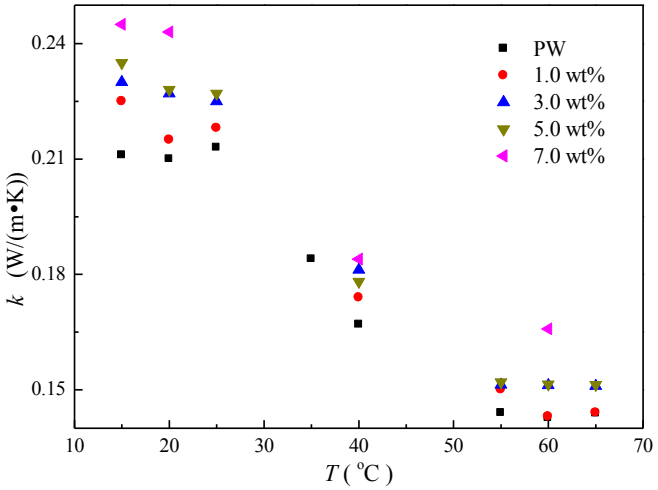

Figure 7 Thermal conductivities of composites vs. temperatures

Figure 7 shows the dependence of thermal conductivity of the composites on temperature for different loadings. The temperature ranges from 15 °C to 65 °C. It is seen that the thermal conductivity of the composites decreases with increasing temperature and phase change. The structure of composite relaxed whenever it experienced a phase change. This is why the thermal conductivity at solid state (15 - 25 °C) is greater than its counterpart at another solid state at 40 °C, and it is lowest at liquid state (55 – 65 °C). At 60 °C, the differences in thermal conductivity between virgin PW and 1.0 wt% composite, and between 3.0 wt% and 5.0 wt% composites are very small.

4 Conclusions

We fabricated TiO_2 nanoparticles and analyzed the particle size and properties by various analytical methods including the SEM, TEM, FTIR and XRD. Results showed the TiO_2 nanoparticles in the anatase form and about 20nm in size. The TiO_2 nanoparticles were added into the melting PW to make TiO_2/PW composites. Through the DSC analysis it revealed that the addition of TiO_2 nanoparticles leads to a minor decrease (≤ 0.5 °C) in solid-solid phase change temperature and an increase (≤ 2.8 °C) in solid-liquid phase change temperature. Both the latent capacities of solid-solid phase change and solid-liquid phase change in the composites reduce, compared with the virgin PW, except for the composite with 1.0 wt% TiO_2 nanoparticles loading in which the latent capacities are enhanced. The TiO_2/PW composites have an enhanced thermal conductivity compared to the virgin PW, and the thermal conductivity increases with the increase of TiO_2 nanoparticles

loading, but decrease with increasing temperature and phase change. The TiO_2/PW composites have a lower thermal conductivity in the liquid state than in the solid state.

Acknowledgments

This work was supported by the National Natural Science Foundation of China (No.51176106, 51306108), and Program for Professor of Special Appointment (Eastern Scholar) at Shanghai Institutions of Higher Learning. Jifen Wang acknowledges the Visiting Scholarship from Shanghai Municipal Education Commission for her stay at Rutgers University from July 2012 to July 2013.

References

[1] Abareshi M, Sajjadi SH, Zebarjad SM, Goharshadi EK. Fabrication, characterization, and measurement of viscosity of alpha-Fe2O3-glycerol nanofluids. Journal of Molecular Liquids 2011;163(1):27-32.

[2] Abdel-Hameed SAM, Margha FH. Preparation, crystallization behavior and magnetic properties of nanoparticles magnetic glass-ceramics in the systems Fe2O3- CoO- MnO2, Fe2O3- NiO-MoO3 and Fe2O3- CoO- V2O5. Journal of Non-Crystalline Solids 2012;358(4):832-38.

[3] Amna T, Hassan MS, Nam KT, Bing YY, Barakat NAM, Khil MS, et al. Preparation, characterization, and cytotoxicity of CPT/Fe2O3-embedded PLGA ultrafine composite fibers: a synergistic approach to develop promising anticancer material. International Journal of Nanomedicine 2012;7:1659-70.

[4] Cheng YH, Kang YF, Wang LW, Wang Y, Wang SR, Li YJ, et al. Preparation of porous alpha-Fe2O3-supported Pt and its sensing performance to volatile organic compounds. Journal of Natural Gas Chemistry 2012;21(1):11-16.

[5] Carkaci-Salli N, Battula S, Wang X, Connor JR, Vrana KE. Gender-specific regulation of tyrosine hydroxylase in thymocyte differentiation antigen-1 knockout mice. Journal of Neuroscience Research 2012;90(8):1583-88.

[6] Cannio M, Bondioli F. Mechanical activation of raw materials in the synthesis of Fe2O3-ZrSiO4 inclusion pigment. Journal of the European Ceramic Society 2012;32(3):643-47.

[7] Zhang DM, Zang CH, Zhang YS, Han YH, Gao CX, Yang YX, et al. Electrical property of nanocrystalline gamma-Fe2O3 under high pressure. Physica B-Condensed Matter 2012;407(6):1044-46.

[8] Johnston JH, Grindrod JE, Dodds M, Schimitschek K. Composite nano-structured calcium silicate phase change materials for thermal buffering in food packaging. Current Applied Physics 2008;8(3-4):508-11.

[9] Wang JF, Xie HQ, Li Y, Xin Z. PW based phase change nanocomposites containing gamma-Al(2)O(3). Journal of Thermal Analysis and Calorimetry 2010; 102(2):709-13.

[10] Fan G, Li H, Cao L, Shan F. Preparation and thermal properties of form-stable palmitic acid/active aluminum oxide coposites as phase change materials for latent heat storage, Materials Chemistry and Physics 2012; 137(9): 558-564.

[11] Keblinski P, Phillpot S R, Choi S U S, Eastman J A. Mechanisms of heat flow in suspensions of nano-sized particles (nanofluids), Int. J. Heat Mass Transfer 2002; 45(4): 855-863.

[12] Doroodchi E, Evans TM, Moghtaderi B. Comments on the effect of liquid layering on the thermal conductivity of nanofluids, J. Nanopart. Res. 2009; 11(6): 1501-07.

[13] He Y, Jin Y, Chen H, Ding Y, Cang D, Lu H. Heat transfer and flow behaviour of aqueous suspensions of TiO2 nanoparticles (nanofluids) flowing upward through a vertical pipe. International Journal of Heat and Mass Transfer 2007; 50(11-12):2272-81.

[14] Hamilton RL, Crosser OK. Thermal conductivity of heterogeneous two-component systems. I&EC Fundamentals 1962; 1(3): 187-191.

[15] Yu W, Choi SUS. The role of interfacial layers in the enhanced thermal conductivity of nanofluids: A renovated Hamilton–Crosser model. Journal of Nanoparticle Research 2004;6(3): 355-361.

[16] Murshed SMS, Leong KC, Yang C. Investigations of thermal conductivity and viscosity of nanofluids. International Journal of Thermal Sciences 2008;47(5):560-68.

[17] Xie HQ, Wang JC, Xi TG, Liu Y, Ai F, Wu QR. Thermal conductivity enhancement of suspensions containing nanosized alumina particles. Journal of Applied Physics 2002;91(7):4568-72.

[18] Murat K, Khamid M. Solar Energy Storage Using Phase Change Materials. Renewable and Sustainable Energy Reviews 2007;11(9):1913-65.

[19] Wang JF, Xie HQ, Xin Z, Li Y, Yin C. Investigation on thermal properties of heat storage composites containing carbon fibers. Journal of Applied Physics 2011;110(9): 094302.

[20] Sarı A. Thermal reliability test of some fatty acids as PCMs used for solar thermal latent heat storage applications. Energy Conversion and Management 2003;44(14):2277-87.

[21] Guo SZ, Li Y, Jiang JS, Xie HQ. Nanofluids Containing gamma-Fe2O3 Nanoparticles and Their Heat Transfer Enhancements. Nanoscale Research Letters 2010;5(7):1222-27.

[22] Nagasaka Y, Nagashima A. Absolute measurement of the thermal conductivity of electrically conducting liquids by the transient hot-wire method. Journal of Physics E: Scientific Instruments 1981; 14(12): 1435.

[23] Bahar E, Ucar N, Onen A, Wang YJ, Oksuz M, Ayaz O, et al. Thermal and mechanical properties of polypropylene nanocomposite materials reinforced with cellulose nano whiskers. Journal of Applied Polymer Science 2012;125(4):2882-89.

[24] Bariain C, Matias IR, Romeo I, Garrido J, Laguna M. Behavioral experimental studies of a novel vapochromic material towards development of optical fiber organic compounds sensor. Sensor Actuat B-Chem 2001;76:25-31.

[25] Sharma A, Tyagi VV, Chen CR, Buddhi D. Review on thermal energy storage with phase change materials and applications. Renewable and Sustainable Energy Reviews 2009;13:318-45.

[26] Xie HQ, Xi TG, Wang JC. Study on the mechanism of heat conduction in nanofluid medium. Acta Physica Sinica 2003;52(6):1444-49.

[27] Pastoriza-Gallego MJ, Lugo L, Legido JL, Pineiro MM. Rheological non-Newtonian behaviour of ethylene glycol-based Fe2O3 nanofluids. Nanoscale Research Letters 2011;6:1-7.

[28] Younes H, Christensen G, Luan XN, Hong HP, Smith P. Effects of alignment, pH, surfactant, and solvent on heat transfer nanofluids containing Fe2O3 and CuO nanoparticles. Journal of Applied Physics 2012;111(6):064308.

[29] Xue Q. Model for effective thermal conductivity of nanofluids. Physics Letters 2003;307:313-17.

[30] Bhattacharya P, Saha S, Yadav A, Phelan P, Prasher R. Brownian Dynamics Simulation to Determine the Effective Thermal Conductivity of Nanofluids. Journal of Applied Physics 2004;95(11):6492-94.